Kovove Mater. 52 2014 19–27
DOI: 10.4149/km_2014_1_19

Effect of process parameters on the microstructure of aluminum alloys obtained by semi continuous casting

C. Méndez[1], C. C. Sánchez[1], E. Salas[1], M. Ríos[1], G. Plascencia[1,2]*, D. Jaramillo[1]

[1] *CIITEC – IPN, Cerrada Cecati s/n México, 02250, D. F. México*
[2] *MSE Department, University of Toronto, 184 College St., Toronto, ON, M5S 3E4 Canada*

Received 19 February 2013, received in revised form 20 September 2013, accepted 8 October 2013

Abstract

Aluminum alloys are processed by semi continuous casting either by direct chill or open mould casting. However, due to intrinsic complications of the casting process and the size of the solidified ingots, it is difficult to evaluate or even predict the effect of process parameters such as cooling water flow rate or casting velocity on the microstructure of the ingots. In this paper we report some results from a laboratory scale built semi continuous machine. Results show that regardless of the casting parameters used, a fine equiaxed microstructure was obtained in every test.

K e y w o r d s: aluminum alloys, solidification, semi continuous casting, microstructure, heat flow

1. Introduction

Semi continuous casting of aluminum (either DC or open mould) is a well established and robust technology used to produce aluminum alloy ingots of different sizes. Once the ingots are obtained, they are sent for further processing steps such as rolling, forging, heat treating among others.

It is desirable to be able to control and predict the microstructure of the ingots as they are cast. This issue becomes more relevant if the physical properties of the products to be manufactured from these ingots must meet a given set of standards.

Due to the size of the ingots, any sort of analysis on either the microstructures or the thermal history of the metal results very expensive and most times impractical to be conducted thoroughly in the cast shop [1, 2].

As pointed out [2–5], cooling systems are largely responsible for the quality of the solidified ingot. Cooling of the ingots is achieved by two cooling systems. The primary cooling system is located in the casting mould itself. The mould has a cavity between its walls so cooling water is passed through. This cooling system is responsible for removing the latent heat of solidification from the melt, so the liquid-solid transformation starts to take place within the mould; in addition, this cooling system removes the sensible heat from the liquid phase. The second cooling system consists of water falling from the lower end of the mould. In the bottom of the mould cavity some holes are drilled alongside the length of the mould so water falls from it in such a way that a water curtain wets the ingot as it is formed and it is also responsible for removing the sensible heat from the already solidified ingot. This secondary cooling system completes the solidification of the ingot and also it cools down the metal.

From the description given above, it is evident that the solidification and therefore the final properties of the alloy cast in this way, strongly depend on parameters such as water flow rate, casting velocity and the geometry of the ingot [6]. Additionally, it is expected that the chemical composition of the casting alloy will also influence such process parameters.

In order to evaluate the effect of such process parameters on the microstructure of the cast alloy, we have built a laboratory scale open mould casting machine to simulate in plant operational conditions. The aim of the project is to evaluate the microstructure of the

*Corresponding author: tel.: 5255 5729 6000 xt 68319; fax: 5255 5729 6000 xt 68319;
e-mail address: g.plascencia@utoronto.ca

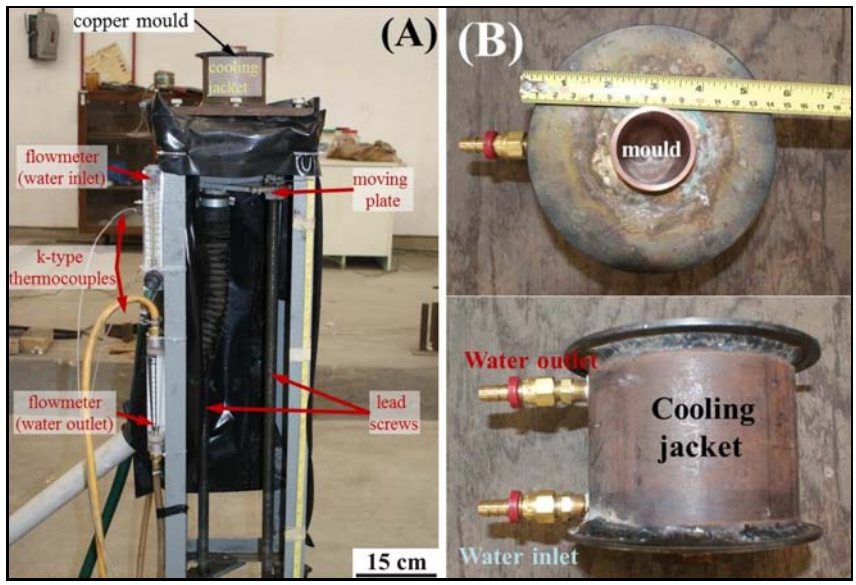

Fig. 1. Experimental setup: (A) picture of the assembled casting machine, (B) details of the mould.

ingots produced in this machine and relate them to the cooling conditions used in plant.

2. Experimental

2.1. Apparatus description

A semi-continuous casting machine was built in our laboratory. The caster essentially consisted of a frame made from low carbon steel. The transmission mechanism consisted of a pulley connected to a couple of lead screws through a series of gears; this mechanism was welded to the caster structure. The pulley was connected by means of a band to a 220 V three phase motor which in turn was controlled with a frequency changing device. Such device allowed for changing the casting speed as well as the direction of the casting plate motion (upwards or downwards). Apart from the mechanical elements of the caster, a copper mould was used to form the aluminum bars, this mould is a cylinder with 5 cm in diameter, 15 cm in length and thickness of 2 mm. The mould was mounted into a low carbon steel jacket. The jacket is a hollow cylinder with 10 cm in length and 15 cm in inner diameter. In addition, two water ports were added to the jacket, one for the entrance of cooling water and the second for removing it. Water was introduced into the jacket at different flow rates. Below the mould/jacket assembly, a metallic support base was placed; under this base a secondary cooling system was added. The secondary cooling system consisted of a 7.5 cm in diameter ring made of copper pipe with inner diameter of 6.4 mm; seven holes (0.08 cm in diameter) were drilled on the inner surface of the copper ring so water could be sprayed over to the surface of the aluminum bars as they were casted. Figure 1A shows a photograph of the casting machine, while Fig. 1B shows a couple of detailed images of the mould.

The casting machine was instrumented with a couple of flowmeters, one for the entrance of water into the jacket, and the second one for the water outlet; the first flowmeter was attached to a valve, so the water inlet flow rate was controlled. A third flowmeter was used to measure the water inlet to the secondary cooling; this flow rate was not controlled. The temperature of the water at the entrance and outlet of the cooling jacket was continuously recorded by means of two k-type thermocouples placed on each port. The thermocouples were connected to a data acquisition system which in turn was hooked to a PC. A third thermocouple was placed into the bottom end of the mould before the metal was cast. This thermocouple measured and registered the temperature of the aluminum as it solidified while passing through the mould and the secondary cooling system. Finally a fourth thermocouple was placed into the crucible in which the aluminum was melted. Temperature data from each thermocouple was recorded every second. To melt the aluminum, an induction furnace was used.

2.2. Materials

The tests conducted consisted on melting aluminum alloys from the 1100, 3004 (wrought) and 332.0 (cast) series in an induction furnace. The metal was placed into a graphite crucible. Once melted, the aluminum was poured into the mould when the melt reached a temperature of 695 °C ± 10 °C. In the case of the 332.0 casting, the metal was poured at 600 °C

Table 1. Chemical composition of the alloys used in this work

Alloy	Composition	Si (wt.%)	Fe (wt.%)	Cu (wt.%)	Mn (wt.%)	Mg (wt.%)	Zn (wt.%)	Ti (wt.%)	Al (wt.%)
1100	Nominal	0.95 max		0.05	0.03		0.1		99.00
	Measured	*0.27*	*0.41*	*0.08*	*0.05*	*0.04*	*0.1*	*0.03*	*99.00*
3004	Nominal	0.30	0.70	0.25	1.00	1.00	0.25		96.00
	Measured	*0.18*	*0.60*	*0.12*	*1.05*	*0.85*	*0.25*		*96.95*
332.0	Nominal	9.5	1.2	3.0	0.5	1.0	1.0	0.25	83.00
	Measured	*8.63*	*0.57*	*2.35*	*0.1*	*0.88*	*0.49*	*0.035*	*86.4*

Table 2. Cooling rates under different experimental conditions

Test	Alloy	Cooling water flow rate ($l\,min^{-1}$)	Cooling water flow rate in secondary ($l\,min^{-1}$)	Casting temperature (°C)	Casting velocity ($cm\,min^{-1}$)	Cooling rate (°C min^{-1})
1	1100	9.5	7.5	697	8.1	–1579
2	1100	9.5	7.5	690	12.5	–1538
3	1100	9.5	7.5	691	17.0	–1521
4	1100	9.5	7.5	693	24.0	–1510
5	1100	9.5	7.5	686	42.0	–1656
6	1100	5.0	7.5	688	24.0	–1585
7	1100	2.0	7.5	688	24.0	–1635
8	1100	2.0	7.5	685	42.0	–1513
9	3004	2.0	7.5	704	42.0	–1827
10	332.0	2.0	8.5	504	42.0	–584

± 10 °C. The chemical composition was not modified; commercial alloys were used in this research, their nominal [7] and actual compositions are shown in Table 1.

2.3. Test description

Before starting the motor to move the caster plate, nearly 0.5 cm of aluminum was allowed to solidify in the mould and then the plate was allowed to move downwards at a predefined casting speed. As the plate moved downwards, the aluminum kept filling the mould. The caster was stopped when the metal left the mould from its lower end completely solidified.

A total of 10 tests were conducted in the apparatus shown in Figs. 1A,B. Table 2 summarizes the different tests conducted. Once the bars were obtained, they were cut into halves alongside its axis; one half of the bar was initially macro etched for visual inspection. Once etched, the half was cut into 5 sections equally sized, taking only 3 of them (beginning, centre and end of the casting). These three sections were prepared for microscopic examination using common metallographic procedures. The second half of the bar was kept as a reference material.

3. Results and discussion

3.1. Cooling rates

Figures 2A,B show plots of temperature vs time for the different bars cast. It is clear from Figs. 2A,B that samples from the 1100 alloy cooled at practically the same rate in spite of being cooled under different conditions, with exception of bar 8. The anomalous behaviour exhibited by bar 8 at the beginning of the casting can be attributed to some motion of the thermocouple, since in this particular test, we placed the thermocouple after we started pouring the aluminum (in the other tests, we first placed the thermocouple and then poured the melt). However, it is evident that towards the end of the casting, this bar cooled at a rate similar to the other bars.

For bars 9 and 10, there is a significant difference between their cooling rates. In the case of bar 9 (alloy 3004), the cooling rate is fairly similar than those shown by bars 1 to 8. On average, the bars from the 1100 alloy cooled at –1567 °C min^{-1}, while bar 9 exhibited in just one test a cooling rate of –1827 °C min^{-1}.

In the case of the 332.0 alloy (bar 10), it cools at a rate considerably slower than the other two alloys. This can be attributed to the high silicon content of 8.6 wt.%. The eutectic in Al-Si alloys occurs at 577 °C

Table 3. Heat balance for each casting experiment

Test	Cast bar weight (kg)	Casting time (min)	Heat released by aluminum (J)	Heat absorbed by cooling water (J)	Casting velocity ($cm\,min^{-1}$)	Water inlet flow rate ($l\,min^{-1}$)
1	0.94	1.00	3.68×10^5	1.91×10^5	8.1	9.5
2	0.64	0.70	2.50×10^5	2.53×10^5	12.5	9.5
3	0.78	0.90	3.05×10^5	2.86×10^5	17.0	9.5
4	0.90	0.81	3.52×10^5	3.54×10^5	24.0	9.5
5	0.44	0.35	1.72×10^5	1.85×10^5	42.0	9.5
6	0.86	1.07	3.40×10^5	3.36×10^5	24.0	5.0
7	0.90	1.83	3.52×10^5	3.60×10^5	24.0	2.0
8	0.92	1.20	3.60×10^5	2.47×10^5	42.0	2.0
9	0.34	0.85	1.33×10^5	6.68×10^4	42.0	2.0
10	0.48	1.20	7.87×10^4	1.08×10^5	42.0	2.0

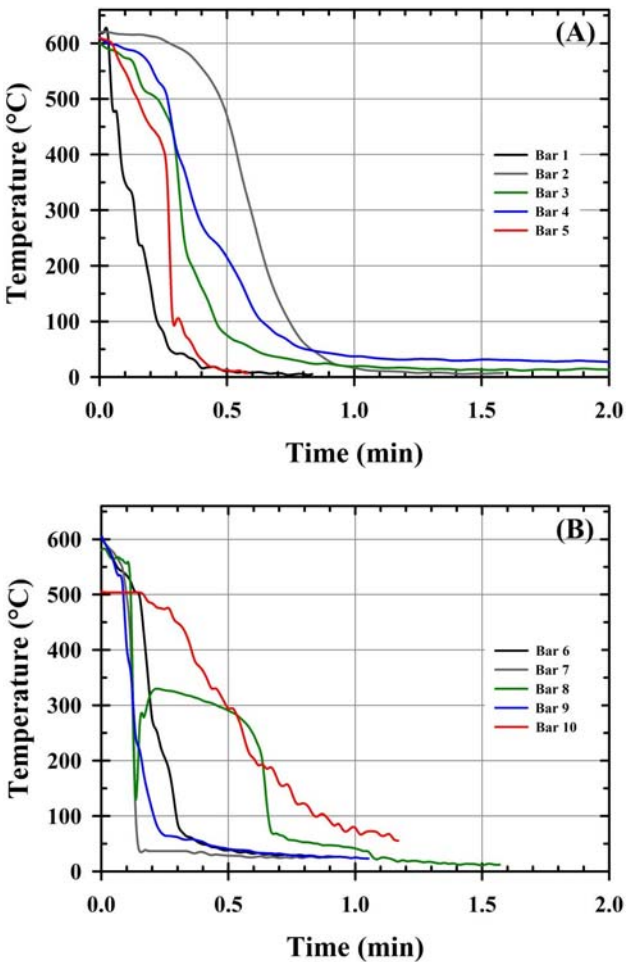

Fig. 2. Cooling of aluminum bars under different experimental conditions: (A) bars 1 to 5, (B) bars 6 to 10.

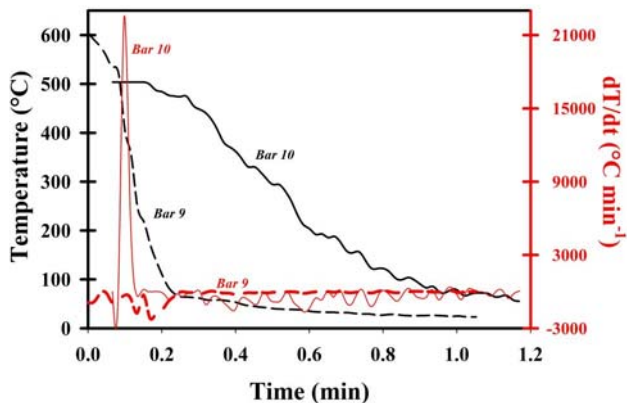

Fig. 3. First derivative of temperature with respect to time of the cooling data for bars 9 and 10.

and 12.6 wt.% Si. Since composition of this alloy is close to the eutectic, it requires less energy to solidify, hence the slower heat removal rate. Another feature that can be appreciated in the cooling curve of ingot 10 is that the liquid-solid transformation is evident at the beginning of the curve. Such transformation cannot be observed in the cooling curves for bars 1 to 9 as clearly as it is for test 10.

Figure 3 shows the first derivative of temperature respect of time for bars 10 and 9; it is evident from this figure the liquid-solid transformation for bar 10 (Al-Si alloy), whereas for bar 9 (alloy 3004) such phase change is not as notorious.

The cooling rates estimated for the different experiments are shown in Table 3. In view of these values, it is possible to say with exception of test 10, that under different experimental conditions, the casting of alloys 1100 and 3004 practically occurs under steady state conditions, i.e., $\frac{\partial T}{\partial t}$ = constant. With this assumption, it is possible to describe the heat transfer during the solidification of an ingot in a continuous or semi-continuous machine in just one dimension, since the z coordinate can be related to the casting velocity through the casting time. For instance, in the case of cylindrical coordinates, which is our case, heat from

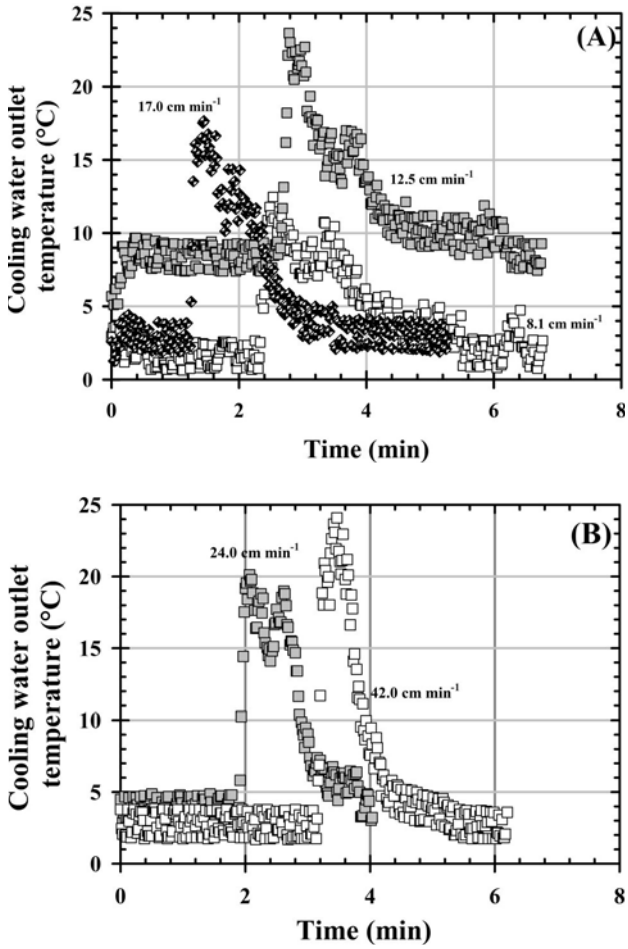

Fig. 4. Effect of casting velocity on cooling water temperature increase: (A) casting at 8.1, 12.5 and 17.0 cm min^{-1}, with water flow rate of 9.5 l min^{-1}; (B) casting at 24.0 and 42.0 cm min^{-1}, with water flow rate of 9.5 l min^{-1}.

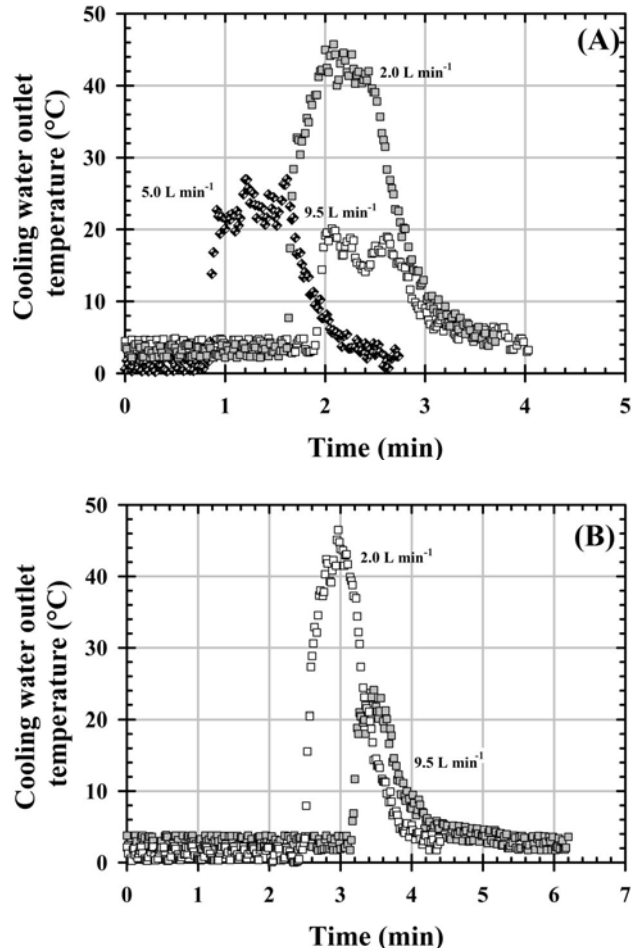

Fig. 5. Effect of water flow rate on cooling water temperature increase: (A) casting at 24.0 cm min^{-1}, (B) casting at 42.0 cm min^{-1}.

the melt is removed solely by the radial coordinate whereas the heat removed in the z direction is negligible. This issue will be addressed in one of the following sections.

3.2. Effect of casting velocity

Tests 1 to 5 were conducted with constant cooling water inlet flow rate at 9.5 l min^{-1}; in these experiments, the casting velocity was gradually increased from 8.1 to 42 cm min^{-1}. By casting at a faster rate, the residence time of the aluminum within the mould decreases. Consequently, when the casting velocity is increased, the water temperature at the cooling water outlet has to increase proportionally. Figures 4A,B show such effect.

It was also observed that the cooling water outlet temperature increment does not correlate directly with the casting velocity. The maximum outlet temperature recorded is 24 ℃ when casting at 12.5 and 42.0 cm min^{-1}. In the case of casting the aluminum at 24 cm min^{-1}, the maximum water outlet temperature reaches 20 ℃, while when casting at 17 cm min^{-1}, the water outlet temperature increases up to 18 ℃. Casting at 8.1 cm min^{-1} results in an increment of the cooling water up to 13 ℃. Similarly, the values of the recorded average temperature increments show a similar increasing trend.

The scatter in the data shown in Figs. 4A,B can be attributed to the water flow turbulence in the cooling jacket.

3.3. Effect of cooling water flow rate

Another set of tests was designed to evaluate the effect of the water flow rate in the mould under a fixed casting velocity. These tests were conducted at casting velocities of 24 and 42 cm min^{-1}, only the 1100 alloy was used in these tests. The cooling water inlet flow rate was increased from 2 to 9.5 l min^{-1}. Results from these experiments are shown in Figs. 5A and 5B, respectively.

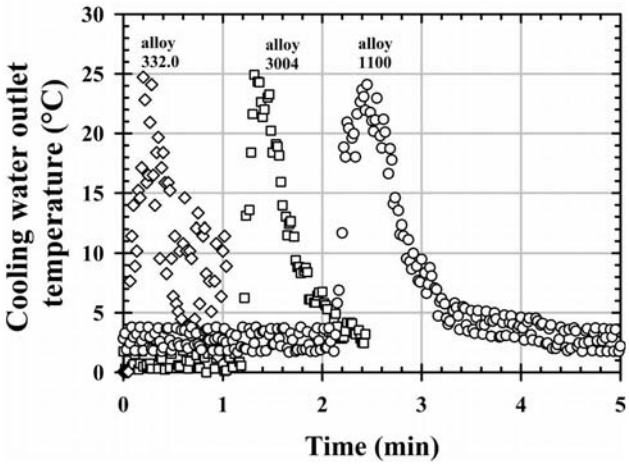

Fig. 6. Effect of chemical composition on the cooling of aluminum alloys (casting velocity 42 cm min^{-1}, cooling water flow rate 2 l min^{-1}).

Figure 5A shows the data recorded for casting the 1100 aluminum alloy at 24 cm min^{-1}; it is evident from this figure that by increasing the cooling water flow rate, the temperature of the water at the outlet port decreases quite dramatically. As more water is passed through the cooling jacket, it is more difficult to heat up this larger volume of water with the heat extracted from the molten metal first and then during the cooling of the resulting bar. In addition, as more water is used for cooling purposes, the faster it needs to leave the jacket, therefore, the more unlikely that the water could absorb the heat coming out of the aluminum. This behavior is also observed in the bars cast at 42 cm min^{-1} (Fig. 5B). By increasing the casting velocity it can be seen in Fig. 5B that the increase in the outlet temperature does not change significantly with respect of casting at 24 cm min^{-1}.

3.4. Effect of chemical composition

The effect of chemical composition is illustrated in Fig. 6. It can be seen in this figure that the cooling water temperature heats up to 25 ℃ regardless of the cast alloy. This effect can be attributed to the similar masses employed in the casting of these alloys. The fact that the cooling water reaches a similar temperature for the different tests means that the amount of heat released by either alloy during its solidification is essentially the same.

In the case of the 332.0 alloy, which has the lowest aluminum content and melting point of the different alloys tested: its data show that the heat removed by the cooling water is basically the same as that released by the alloys with higher aluminum content. This particular result is important in terms of the heat balance. The 332.0 alloy is an Al-Si alloy whose composition nears the eutectic temperature at 577 ℃, this means that this alloy has to be cast at least at 600 ℃; by comparison, the 3004 alloy contains 96 wt.% Al and its melting point is around 660 ℃, thus this alloy is cast at least at 680 ℃. This means that there is a minimum casting temperature difference of 80 ℃ between these alloys and hence much more energy has to be supplied to the 3004 alloy in order to melt and pour properly. However, the data obtained show that the same amount of energy is delivered by both alloys. Unfortunately, the lack of data on latent heat of solidification and heat capacity of the 332.0 complicates a proper heat balance of this alloy, making it difficult for a direct comparison with the heat balance for alloy 3004.

3.5. Heat balance

The amount of heat absorbed by the cooling water within the mould was estimated by means of the equation:

$$q_{\text{water}} = \dot{Q}_{\text{water}} \cdot \rho_{\text{water}} \cdot \text{Cp}_{\text{water}} \cdot \Delta T_{\text{water}} \cdot t_{\text{casting}}, \quad (1)$$

where q_{water} is the amount of energy removed from the molten aluminum by the cooling water (J), $\dot{Q}_{\text{water}}$ is the cooling water flow rate (l min^{-1}), ρ_{water} is the density of water (1000 kg m^{-3}), Cp_{water} is the heat capacity of water (4180 J kg^{-1} K^{-1}), ΔT_{water} is the cooling water temperature difference between the inlet and outlet ports (K), and t_{casting} is the time in which the casting proceeded (min).

This amount of energy removed by the cooling water has to be equivalent to that released by the molten aluminum as it solidifies. To account for the heat lost by the aluminum it is necessary to assume both the 1100 and 3004 alloys as pure aluminum. Unfortunately, this assumption cannot be done for the 332.0 alloy considering its aluminum content.

The heat lost by the melt is divided in terms of the latent heat of solidification and the sensible heat lost from the pouring temperature to that of the phase change. This amount of energy is given by:

$$q_{\text{Al}} = q_{\text{latent}} + q_{\text{sensible}} \quad (2)$$

and

$$q_{\text{latent}} = m_{\text{cast}} \cdot \Delta H^{\circ}_{\text{solidification}}, \quad (3)$$

$$q_{\text{sensible}} = \frac{m_{\text{cast}}}{27} \cdot \int_{T_{\text{p}}}^{T_{\text{mp}}} \text{Cp}_{\text{Al,l}} \cdot \text{d}T, \quad (4)$$

where $\Delta H^{\circ}_{\text{solidification}}$ is the latent heat of solidification of aluminum (3.91×10^5 J kg^{-1}), m_{cast} is the

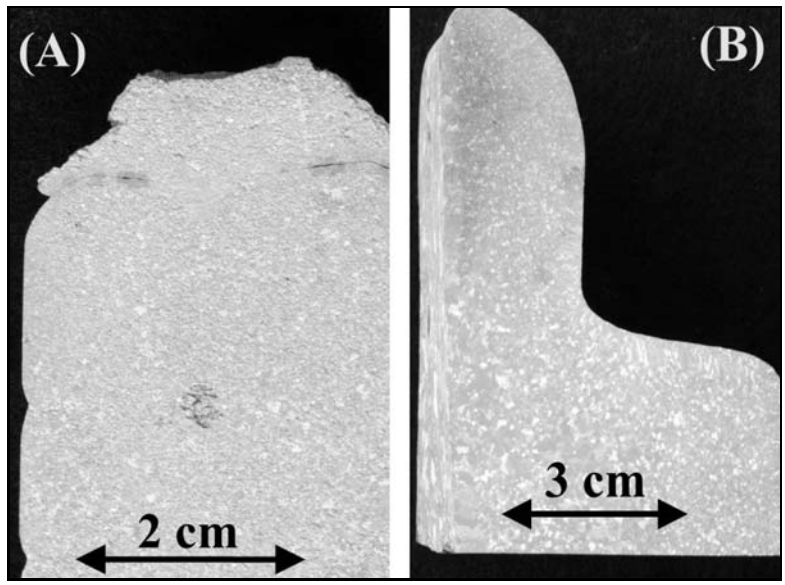

Fig. 7. Macroetch on aluminum alloy 1100 solidified in (A) our laboratory semicontinuous casting machine (bar 1), and (B) permanent iron mould.

mass of the bar casted (kg), $Cp_{Al,l}$ is the heat capacity of the liquid aluminum (31.748 J mol^{-1} K^{-1}), T_{mp} is the melting point of the aluminum (K), and T_p is the pouring temperature (K). Thermophysical data used in Eqs. (1), (3) and (4) were taken from literature [8, 9].

For the 332.0 alloy, the lack of thermophysical data for its solidification made impossible to conduct a proper heat balance, although by using the heat capacity and heat of solidification of pure aluminum and multiplying them by the mass fraction of aluminum, the heat balance for bar 10 was approximated; such balance is shown in Table 3, and it seems to work out favorably. Additionally, it is evident from Table 3 that the heat balance within the mould is fulfilled satisfactorily. The difference between the heat extracted from the water and that released by the aluminum can be explained in terms of the sensible heat from the solidification temperature of the metal to the temperature of the bar as it is removed from the casting machine which not always was the same, therefore that heat contribution was not accounted for.

3.6. Macrostructural evaluation

Once cast, the bars were prepared for metallographic evaluation. A homogeneous structure was found all over the sections. No indication of columnar grain growth was detected. Only equiaxed grains were observed all over the samples obtained.

Figure 7A shows a picture of the macroetch on the 1100 aluminum alloy after being solidified in our casting machine (Test 1), whereas Fig. 7B shows an image of the same aluminum alloy solidified in a permanent iron mould. Figure 7A only shows randomly oriented equiaxed grains with almost the same mean size; on the other hand, Fig. 7B shows the presence of columnar and equiaxed grains. The presence of the columnar grains near the ingot ends is evident; while at the ingot centre and edges, equiaxed grains have developed. The columnar grains also depict the heat flow during solidification in the permanent mould. As expected, heat transfer in the iron mould is more complex than that in the continuous casting machine. In addition, columnar growth is also expected to occur in this kind of solidification due to localized thermal and compositional gradients.

The presence of only equiaxed grains in Fig. 7A confirms the fast heat extraction already described. Additionally, the macrostructural features observed in this figure also indicate that the metal presented little resistance to heat removal in the radial direction. Since aluminum has a relatively high thermal conductivity, plus the action of the cooling flow rate, it allows for rapid and homogeneous solidification by means of a uniform solidification front advancing from the bar centre towards the mould wall. All bars cast in our casting machine showed the same structural features, i.e., homogeneous equiaxed grains randomly distributed all over the bars.

3.7. Microstructural evaluation

Figures 8A–E show microstructures of the bars form the different cast alloys. Equiaxed grain morphology is observed in all cases. For alloy 1100 (Figs. 8A–C), a finer microstructure was obtained at the edge of the samples when compared with the coarser structure observed at its centre. This fact is attributed to the effect of the volume of water used to cool down the melt.

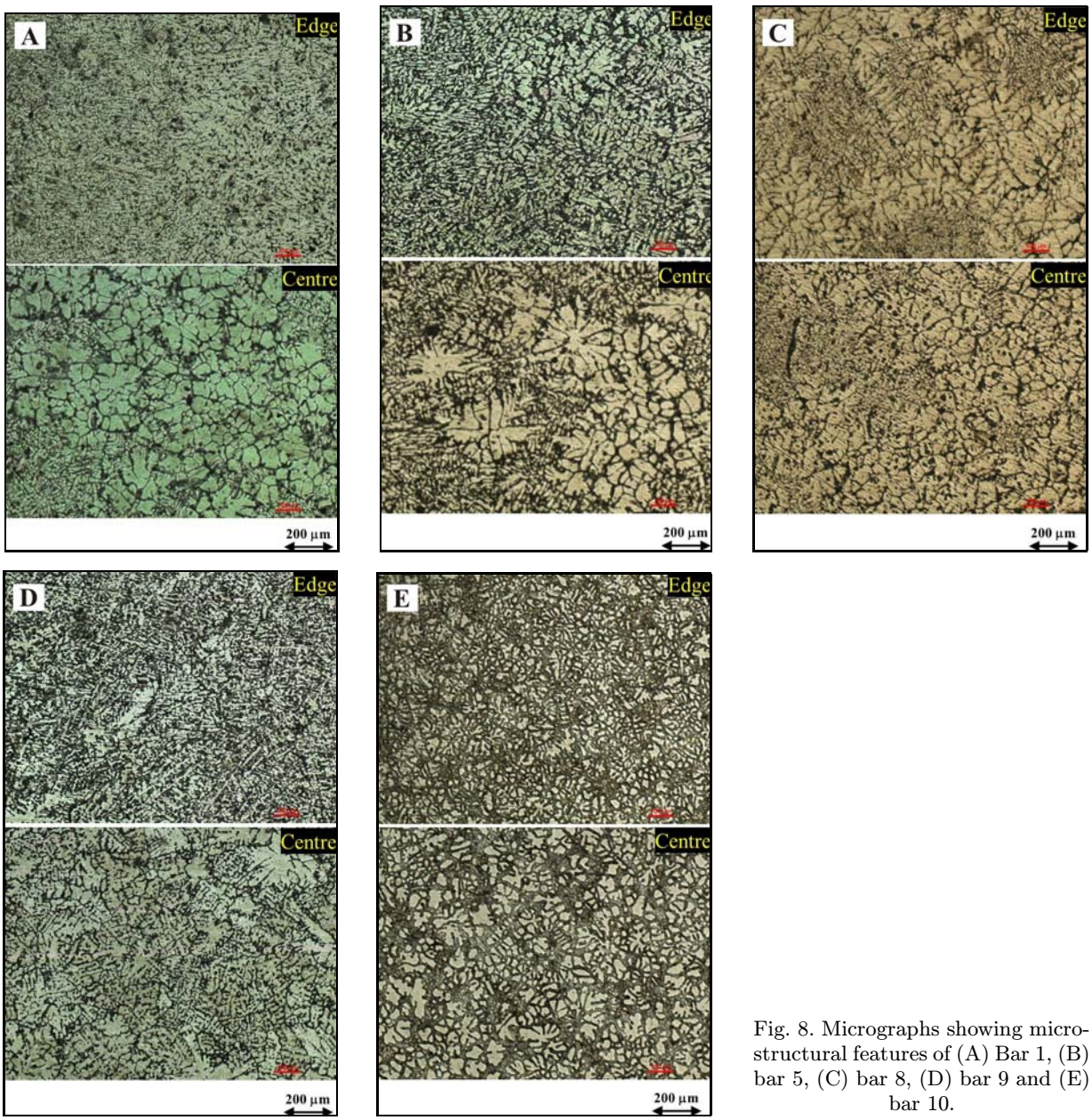

Fig. 8. Micrographs showing microstructural features of (A) Bar 1, (B) bar 5, (C) bar 8, (D) bar 9 and (E) bar 10.

The finer microstructure at the edge of the sample and the coarser one at its centre is also observed in alloy 3004 (Fig. 8D) and alloy 332.0 (Fig. 8E).

In the samples from alloy 1100 it can be noticed that as the water flow decreases, the structure at the edge of the samples is not as fine as those shown by bars cooled with a larger volume of water. Additionally, the process parameters do not seem to affect the microstructure of the different alloys cast. This is evident from the microstructural characteristics (grain size and distribution) of the three alloys despite the difference in chemical composition.

In case of the casting velocity, this parameter seems to be second to the rate of cooling, since there is no significant difference in the structural features of the bars cast at different velocities. This may indicate that the rate of cooling is the most important process parameter in the semicontinuous casting of these alloys.

Nearly pure aluminum (alloys 1100 and 3004) and practically an eutectic alloy (332.0) were used, therefore a well defined liquid-solid interface was expected; thus solidification should take place at a very well established temperature or over a narrow temperature interval. As the solid fraction grows within the mould, the more difficult it becomes for the liquid to flow away. Then, if solidification takes place as fast as our measurements indicate, the more difficult it becomes to develop localized compositional gradients. Furthermore, the relatively high thermal conductivity of aluminum and the high water flow rates employed to so-

lidify the metal enhance the heat transfer which occurs in the radial direction, thus limiting the formation of thermal gradients within the mould yet providing a solid metal shell able to withstand the metallostatic pressure of the melt in the mould. These observations are in agreement with those by Raiszadeh and Esfahani [10].

Shabestari and Malekan [11] have shown that by increasing the cooling rate, all microstructural features of a metal are refined as it solidifies; the addition of a chill enhances the refinement of dendrite structure.

Further questions regarding as to where the solidification front exists may arise as the metal is cast, so it becomes more difficult to establish a smooth phase transformation [12].

4. Conclusions

Experimental work has been conducted to establish the relationship between process parameters and microstructural features in aluminum bars from different alloys processed by semi continuous casting. It has been found that water cooling flow rate is the most important factor that determines the final microstructure of the cast material.

In every case a fine microstructure was found, finer at the edge of the cast samples and coarser at their centre. This type of structure reveals that the aluminum does not present a significant thermal resistance during its solidification, thus allowing the formation of equiaxed grains all over the alloy matrix.

Although the results obtained in this work are positive in terms of predicting the mechanical properties of the alloys processed in the laboratory, still, there is not a clear manner to extrapolate directly our results to ingots cast at a larger size.

Acknowledgements

Financial support from SIP-IPN grants is greatly appreciated. Thanks are also due to Dept. of Metallurgy UASLP for sharing their facilities with us.

References

[1] Meredith, M. W., Worth, J., Brown, J. M., Hamerton, R. G.: In: Proceedings Light Metals 2003. Ed.: Crepeau, P. N. San. Diego, CA, TMS 2003, p. 1111.
[2] Méndez, C., Sánchez, C. C., Plascencia, G., Rubio, M. A., Jaramillo, D.: In: Proceedings Light Metals 2010. Ed.: Johnson, J. A. TMS 2010, p. 715.
[3] Hamer, S.: In: Proceedings Light Metals 2010. Ed.: Johnson, J. A. TMS 2010, p. 709.
[4] Kiss, L. I., Meenken, T., Charette, A., Lefebvre, Y., Lévesque, R.: In: Proceedings Light Metals 2003. Ed.: Crepeau, P. N. San Diego, CA TMS 2003, p. 829.
[5] Sommerhofer, H., Sommerhofer, P.: In: Proceedings Light Metals 2006. Ed.: Galloway, T. J. Warrendale, Pa, TMS 2006, p. 865.
[6] Ni, F., Motoyasu, G., Soda, H., McLean, A.: Int. J. Cast. Met. Res., *22*, 2009, p. 438. doi:10.1179/174313309X449273
[7] ASM Metals Handbook. Vol. 2. 10th Edition. Metals Park, OHASM International 1990.
[8] Bejan, A.: Heat Transfer. New York, Wiley 1993.
[9] Roine, A.: Outokumpu HSC Chemistry V 6.0.
[10] Raiszadeh, R., Bartar Esfahani, H.: Int. J. Cast. Met. Res., *23*, 2010, p. 264. doi:10.1179/136404610X12682097603849
[11] Shabestari, S. G., Malekan, M.: Can. Met. Q., *44*, 2005, p. 305.
[12] Soda, H., McLean, A., Motoyasu, G.: Int. J. Cast. Met. Res., *18*, 2005, p. 163. doi:10.1179/136404605225022973